DEVELOPMENT OF REGIONAL DISCRIMINANTS

Don V. Helmberger and Xi Song
Seismological Laboratory
California Institute of Technology, Pasadena, CA 91125

ABSTRACT

With the installation of broadband, high dynamic range instruments, it has become possible to compare the regional waveforms of earthquakes and explosions at magnitudes 3 to 6. These waveforms are similar for event sequences in many situations and can be inverted for source mechanisms. We find that flat-layered models are sufficient for inverting seismograms at periods greater than a few seconds. This paper presents three studies aimed at determining crustal models, source finiteness and modeling complex structure near a receiver.

We have conducted a set of sensitivity tests on the parameters of 1-D models to compare their impact on different segments of regional seismograms. We found that P_{nl} waves (extended P-waves) are controlled in broadband character by the mid-crust while the top layer contributes to the long-period motions. The *SV* wave is mostly controlled by the shear wave velocity of the lower crust, especially the crustal layer just below the source depth. The top crustal layer controls the shape of the surface waves at ranges from 300 to 600 km, and the upper crust, especially the crustal layer just above the source depth, controls their timing. Applying these tests in modeling three earthquakes in the Basin-and-Range province, we found that a simple two-layer crustal model could effectively explain the data both in timing and in shape. The main crustal layer has *P* and *S* velocities of 6.1 km/sec and 3.6 km/sec, similar to those found by Langston and Helmberger (1974). A surface layer of thickness 2.5 to 3.5 km is required to fit the Rayleigh waves.

Fast estimation of point-source parameters for earthquakes has witnessed much progress in recent years due to the development of broadband seismic networks. The expansion of these networks now provides the opportunity to address second order effects such as source directivity and finiteness for regional and local events on a routine basis. To study the directivity for a finite source, we discretize the fault region into a set of elements represented as point-sources. We then generate the generalized rays for the best-fitting point-source location and derive for each separate ray the response for neighboring point-sources with power series expansions. The total response for a finite fault then becomes a double summation over rays and elements. If we sum over elements first, we obtain an effective far-field source-time function for each ray, which becomes quite sensitive to the direction of rupture. These far-field source-time functions are convolved with the corresponding rays and the results summed to form the total response. A simple application of the above method is demonstrated with the tangential motions observed from the 1991 Sierra Madre earthquake.

A 2-D SH hybrid method was developed, which combines finite-difference applied in the inhomogeneous region and an analytic method, GRT, outside. GRT enables us to study basin effects and complex receiver structure for different types of incident energy. The comparison of hybrid method seismograms, GRT seismograms, and regular finite-difference seismograms yields good agreement.

58

19960624 092

OBJECTIVE

Recent advances in instrumentation allowing low amplitude Rayleigh wave detection coupled with new analytical techniques has demonstrated the capability of inverting regional waveform data for source excitation down to relatively low magnitudes. To achieve this requires the determination of regional crustal models and path calibrations from master events. This approach can be applied in many countries of interest where earthquakes are plentiful and event discrimination is difficult. However, once these models are determined, we still need to address the question of what criterion do we use to distinguish the "first blast"? We propose to address this issue by a detailed study of US explosions and earthquakes as observed in Southern California by nearly 300 short-period stations and TERRAscope. Thus, separating propagation features from true source phenomenon should be greatly aided by the completeness of the observations. That is, we can see observationally what happens to broadband signals as they encounter ridges, valleys, faults, etc. This region is rich in sources with quarry blasts, NTS shots, and many different types of earthquakes, thus providing ample data for definitive testing and the development of regional discriminants.

RESEARCH ACCOMPLISHED

We have examined broadband waveforms from a large number of NTS explosions and earthquakes throughout the southwestern United States in order to characterize seismic sources. Explosions were found to be richer in coda energy than earthquakes. Most earthquakes show relatively little long-period (T>4 sec) coda energy and tend to be richer in long-period and shear-wave energy than explosions. We have developed several seismic discriminants based on these observations and our modeling experience. One promising discriminant is the ratio of short-period vertical component, P-wavetrain energy, to long-period surface wave energy, averaged over three components. Explosions tend to have a higher ratio than do earthquakes, essentially an extension of $m_b:M_s$. Magnitude threshold for this discriminant is about 3.5. Another useful discriminant is based on the total broadband energy to moment ratio where explosions are distinguished by their stronger energy levels relative to their long-period amplitudes. This approach requires Green's functions, a source estimator program, and processes all events as earthquakes. For this method to be effective requires the calibration of the region using relatively large earthquakes, M>5, but does not require calibrations of explosions, see last year's research report and references; Helmberger and Woods (1995), Woods et al., (1993), Woods and Helmberger (1994), Zhao and Helmberger (1995).

In this year's report, we will address three topics involving studies that help refine earthquake source effects (depth, directivity, etc.) and regional modeling of structure. Note that we detect explosions because they do not look like earthquakes.

a) Estimation Of Earthquake Parameters

The approach followed here, Zhao and Helmberger (1995), uses a direct grid search and does not require stable partial derivative of waveforms. This method matches complete broadband observed seismograms against synthetics over discrete phases so that timing shifts between particular arrivals are allowed. This feature desensitizes the crustal model used in generating the synthetic waveforms used.

An application of this procedure is displayed in figure 1 along with depth sensitivity of regional phases versus teleseismic waveforms. In this example, only one station is used to determine the three source parameters which yields various solutions as a function of depth. The solution obtained from TERRAscope is displayed as BB which is at a depth of 10 kms. This depth agrees well with teleseismic depth phases, namely sP as displayed in figure 1. The individual depth phases in the regional data, p^Pm^P, s^Pm^P, s^Sm^S, etc. are quite obvious at higher frequency as pointed out by Helmberger et al., (1992), although they are strongly affected by

source directivity, Dreger and Helmberger (1993). The importance of source directivity is becoming increasingly clear in TERRAscope data, see Song et al., (1995) and others, and methods of estimating these effects by analytical means is discussed by Saikia and Helmberger (1995).

In short, the expansion of broadband networks such as TERRAscope is providing the opportunity to address second order effects such as source directivity and finiteness for teleseismic, regional and local events on a routine basis. Making this practical motivates the development of methods to quickly generate synthetic seismograms for finite sources. This proves possible when the fault dimension is small compared to the source-receiver distance and when the structure around the source region is relatively simple. To study the directivity for a finite source, we discretize the fault region into a set of elements represented as point-sources. We then generate the generalized rays for the best-fitting point-source location and derive for each separate ray the response for neighboring point-sources with power series expansions. The total response for a finite fault then becomes a double summation over rays and elements. If we sum over elements first, we obtain an effective far-field source-time function for each ray, which becomes quite sensitive to the direction of rupture, see figure 2. As displayed in the upper panel, the goodness of fit to a particular record becomes strongly dependent on rupture direction and easily included in source inversion, see Song and Helmberger (1995). These far-field source-time functions are convolved with the corresponding rays and the results summed to form the total response.

b) Crustal structure

The source estimation code used in modeling the regional records such as in figure 1 is used routinely to obtain fault parameters from TERRAscope data, i.e., Jones (1995). It uses a store of Green's functions computed on a range interval of 5 kms, and on a depth interval of 3 kms starting at a depth of 5 km, see last year's Seismic Research Symposium summaries, and Zhao and Helmberger (1995). While the SC model proves effective because of the shifting specialized models or regionalized local models work even better as displayed in figure 3. A simple two-layer crustal model is found for this basin-and-range region that fits the events very well as reported on by Song and Helmberger (1995). To find an average model that fits the data in both absolute time and waveform, we generate broadband reflectivity synthetics and conduct sensitivity tests on different parts of a layered crustal model, where only a few layers are involved. Generalized rays are used to help identify the various phases. It proves useful to decompose a regional seismogram into segments so that the impact of model parameters on each segment is the most direct. Thus, it is established that the top crustal layer controls the Rayleigh wave, the Airy phase, in shape over the range from 300 to 600 km, and the crustal layer just above the source depth controls its timing. The P_{nl} waves, the P_n and P_L portion, are controlled in broadband character by the mid-crust while the top layer contributes to its long period motion. These crustal parameters control the tangential motion similarly. The SV wave, the segment between the P_{nl} wave and the Rayleigh wave, is mostly controlled by the shear velocity of the lower crust. In judging the goodness of fit between the array observations and synthetic waveforms, we allow individual data segments to shift relative to the 1-D synthetics a few seconds to account for some lateral variation. The amount of time shift is found by the cross-correlation in displacement between the data segment and the synthetics. Applying these tests in a forward modeling approach, we find that a simple two-layer crustal model is effective in explaining a Basin-and-Range data set. In this model, the main crustal layer has P and S velocities of 6.1 km/sec and 3.6 km/sec, similar to those found by Langston and Helmberger (1974). A surface layer of thickness 2.5 to 3.5 km is required to fit the Rayleigh waves. The refined model can be used as a reference model for locating source inversions for other events. We find that two-layer crustal models prove effective in many regions, see Zhu and Helmberger, and Woods and Saikia of this report.

60

c) Analytical and Numerical Interfacing

Our present regional source estimator program works reasonably well because it allows for lateral variation. This is achieved by allowing small shifts in timing between phases. Some physical basis for this rather ad hoc procedure is given in figure 4, where we display the effects of 2-D structures. Model (a) is a typical 1-D Southern California structure. Model (b) is similar to (a) but with the addition of a soft surface structure (basin-like materials). Models (c) and (d) contain basins in the source region. The synthetics are the most similar on the vertical component, especially (a), (c) and (d). Thus, we can roughly predict (c) and (d) from (a) by slightly separating the P-wave from the Rayleigh wave. The source code handles this nicely in its present form. The radial component does not work so well both in waveform and amplitude. The Love-wave portion of the tangential motion is not very well developed at this range but we can still see a shift developing. Thus, we can add this feature to the code by generating the Love-wave (top structure), as discussed in Helmberger et al., (1992), and shifting the bodywaves separately.

Another important issue is how to treat local scattering near the receiver. This is very important at the shorter periods and we probably need help from other investigators to do this right. However, one possible approach is to treat the receiver as a separate operator and introduce a separate structure at the receiver. Figure 5 displays such a procedure, where we can propagate the field analytically up to the receiver and introduce a local structure. Since finite-differencing does not need to propagate far, this becomes a viable approach. The method would allow us to model some of the obvious shifts in radial vs. vertical Rayleigh waves and their strange amplitude ratios. We could also use this technique to account for high frequency energy enhancement at particular stations that is commonly observed.

RECOMMENDATIONS

In the calibration of new regions, we must develop some "master events" which are well recorded teleseismically, and thus their source parameters can be determined. The regional records of these known events can then be used to develop the local structure, Zhao and Helmberger (1993), and others. This approach seems to work but for small events in isolated regions with only a few regional records, it would be useful to include other short-period array stacks of the P-waves (say, first 50 secs), especially if the event can be seen teleseismically. Thus, we recommend better communication links between array processors and waveform source estimators.

REFERENCES

Dreger, D. S. and D. V. Helmberger (1993). Determination of Source parameters at Regional Distances with Three-Component Sparse Network Data, *J. Geophys. Res.*, **98**, No. B5, 8107-8125.

Helmberger, D. V., and B. B. Woods (1995). Regional Source Parameters, Seismic Energy, and Discrimination, Proceedings in the NATO ASI Conference, Series E, Alvor, Portugal.

Helmberger, D. V., D. Dreger, R. Stead, and H. Kanamori (1992c). Impact of broadband seismology on strong motion attenuation, *Bull. Seism. Soc. Am.*, **83**, 830-850.

Jones, L. Part I: Broadband modeling of aftershocks from the Joshua Tree Landers and Big Bear sequences, Southern California. Part II: Characteristics of the June 28, 1992, Big Bear mainshock from TERRAscope data: evidence for a multiple event source, Ph.D. Thesis, Caltech, Pasadena, CA, June 1995.

Langston, C. A. and D. V. Helmberger (1974). Interpretation of Body and Rayleigh waves from NTS to Tucson, *Bull. Seism. Soc. Am.*, **64**, 1919-1929.

Saikia, C. K. and D. V. Helmberger (1995). An algorithm to compute-up and down-going wavefields for seismic sources, submitted to *BSSA*.

Song, X. J. and D. V. Helmberger (1995). Broadband modeling of regional seismograms; constraints on Basin and Range crustal structure, Spring Abstr., SSA (in preparation).

Song, Xi, L. Jones, and D. V. Helmberger (1995). Source characteristics of the January 17, 1994 Northridge, California earthquake from regional broadband modeling, *BSSA* (in press).

Wen, L., C. Scrivner, and D. V. Helmberger (1995). 2-D SH Hybrid method study of the Los Angeles Basin effects (in preparation).

Woods, B. B., S. Kedar, and D. V. Helmberger (1993). M_L:M_O as a Regional Seismic Discriminant, *Bull. Seism. Soc. Am.*, **83**, 11677-11683.

Woods, B. B. and D. V. Helmberger (1994). Regional Seismic Discriminants using Wavetrain energy ratios, submitted to *BSSA*.

Zhao, L. S. and D. V. Helmberger (1993). Source retrieval from broadband regional seismograms: Hindu Kush region, *Phys. of the Earth and Planet. Inter.*, **78**, 69-95.

Zhao, L. S. and D. V. Helmberger (1994). Source estimation from broadband regional seismograms, *Bull. Seism. Soc. Am.*, **84**, 91-104.

Zhao, L. S. and D. V. Helmberger (1995). Regional Moments, Energy Levels, and a New Discriminant, submitted to *BSSA* (in press).
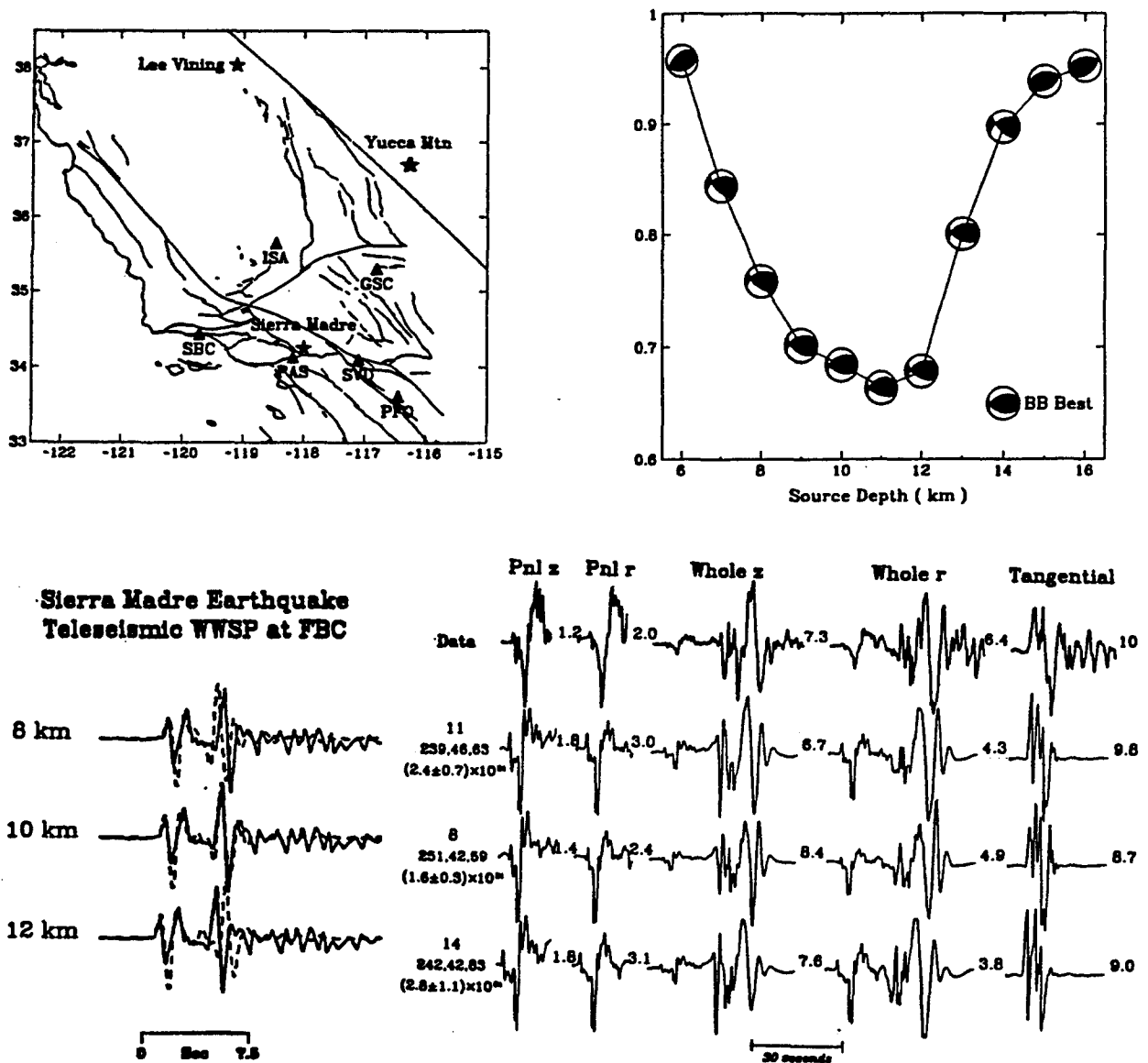
Figure 1. Results from modeling the Sierra Madre Earthquake as displayed in the upper corner. Comparison of synthetics and data at teleseismic distant (FBC, short-period waveforms displaying P and sP) and regional (GSC, $\Delta = 160$ kms, three components). The plot in the upper right hand corner displays the sensitivity (error vs. depth) and the corresponding mechanisms.
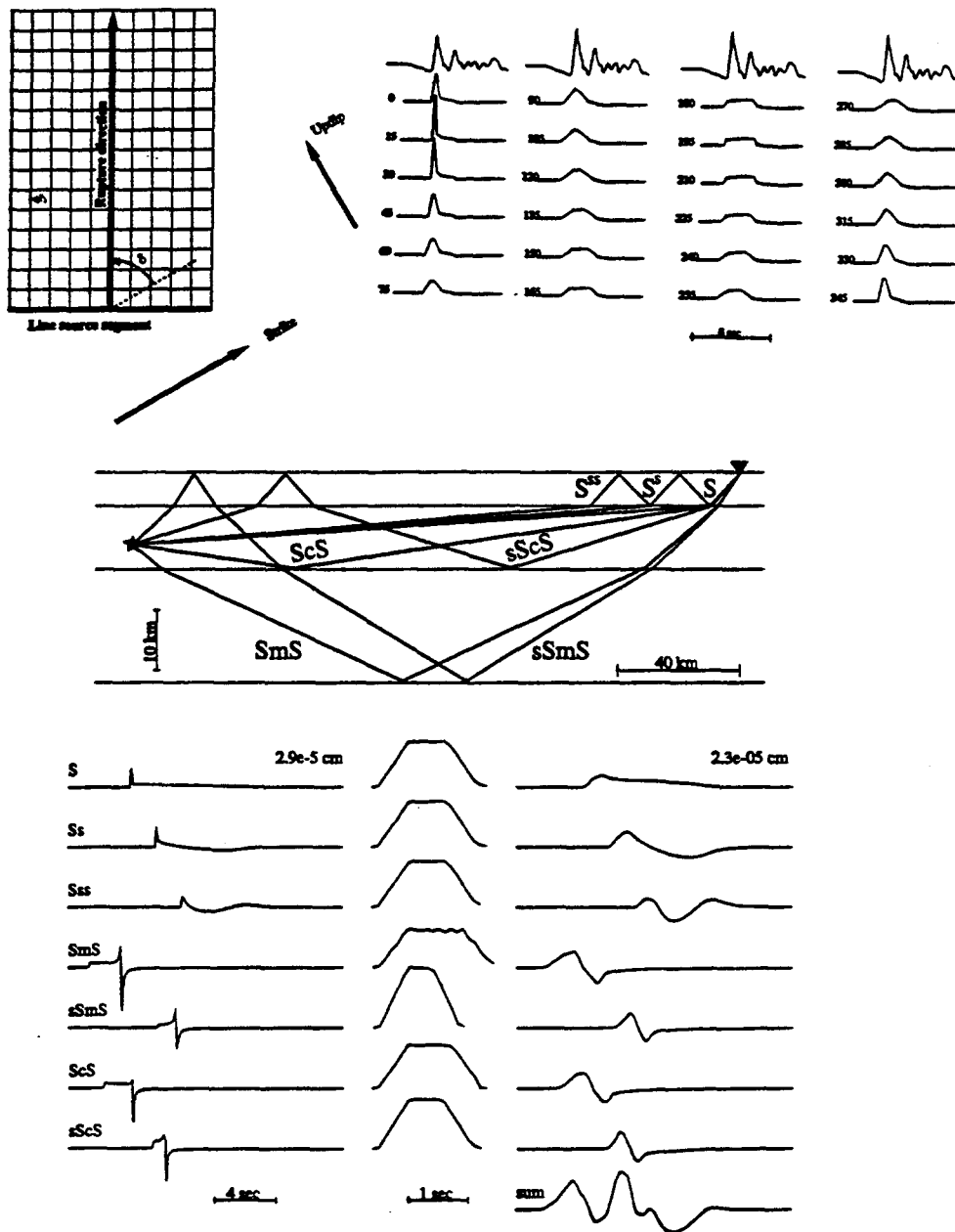
Figure 2. The upper panel (left) displays a map view of a discretized fault. Rupture is simulated by a line source segment propagating perpendicular to itself. The rupture angle δ is defined here to specify the rupture direction. When calculating the synthetic seismograms, each element of the fault is represented by a point-source with a weighting factor w_j. Upper panel (right) displays the comparison between data (PAS, tangential motion, the first trace in each column) and synthetics for fault size 5 x 5 km and varying rupture angles. Seismograms in each column are aligned in absolute timing and scaled with respect to peak amplitude. Numbers indicate rupture angles. Middle panel shows paths of some of the important rays. The star indicates the source and the triangle indicates the receiver. The lower panel displays the ray responses (left column, displacement) and the corresponding unit-area far-field source-time functions (middle column). Each ray is convolved with its corresponding far-field source-time function and the results (right column) are summed to form the total response (the right bottom trace) from the complex source. In this example, a 3-km-long line source segment propagates 2 km up-dip from a depth of 12 km at a constant velocity 3.0 km/sec on a fault plane striking 242° and dipping 50°. Source-receiver distance is 200 km and the station azimuth is 44°. Seismograms are scaled by peak amplitude. A source-time function (0.1, 0.1, 0.1) is used for each point-source, after Song & Helmberger (1995).
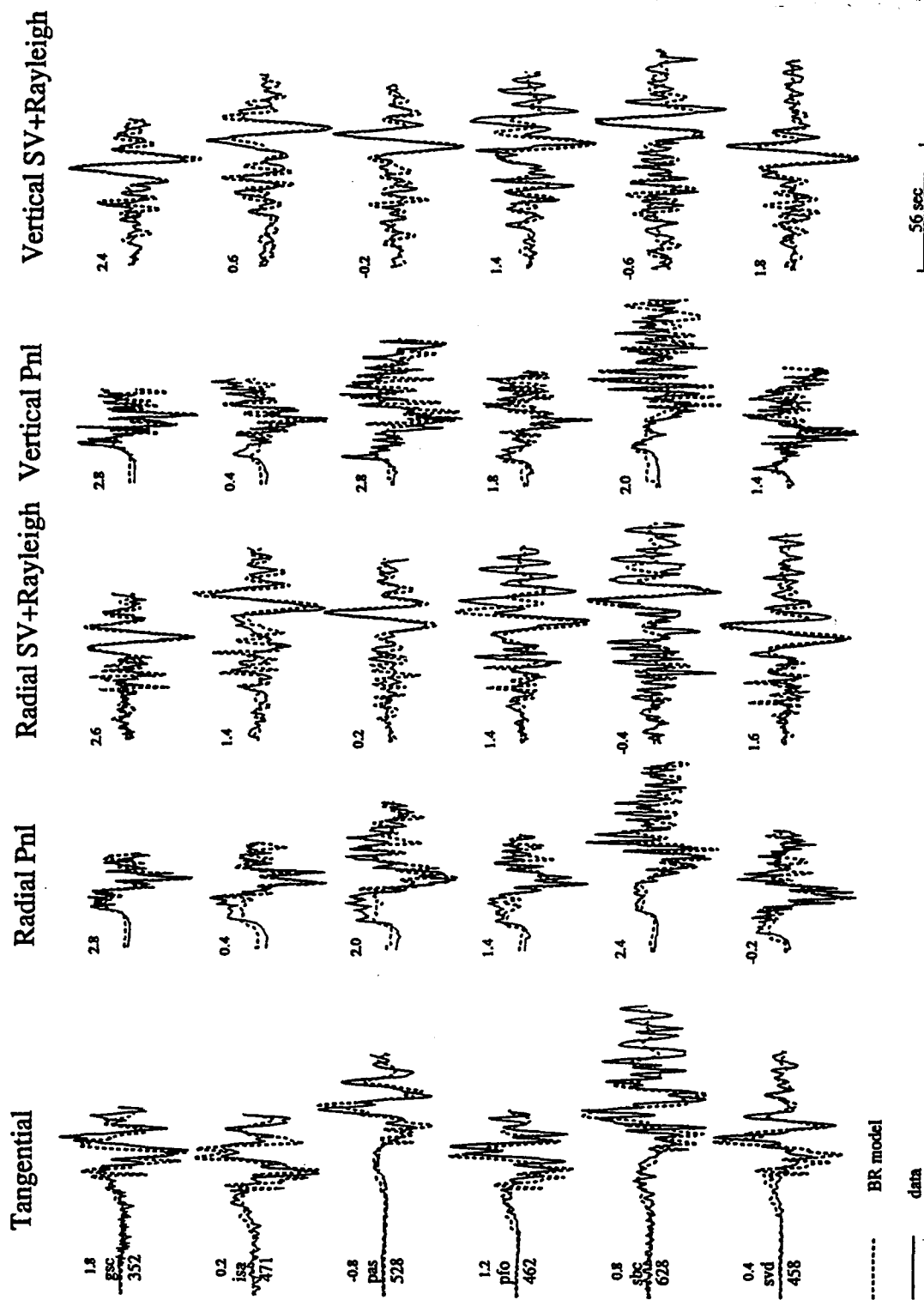
64

Figure 3. Comparison between data and synthetics (2-layer model) for a Utah event, Song and Helmberger (1995). The P-velocities are 3.6, 5.8, 7.85; the S-velocities are 2.05, 3.57, 4.53; thicknesses are 2.5 and 32.5 km. The numbers indicate the relative shift of the synthetic to align with data.
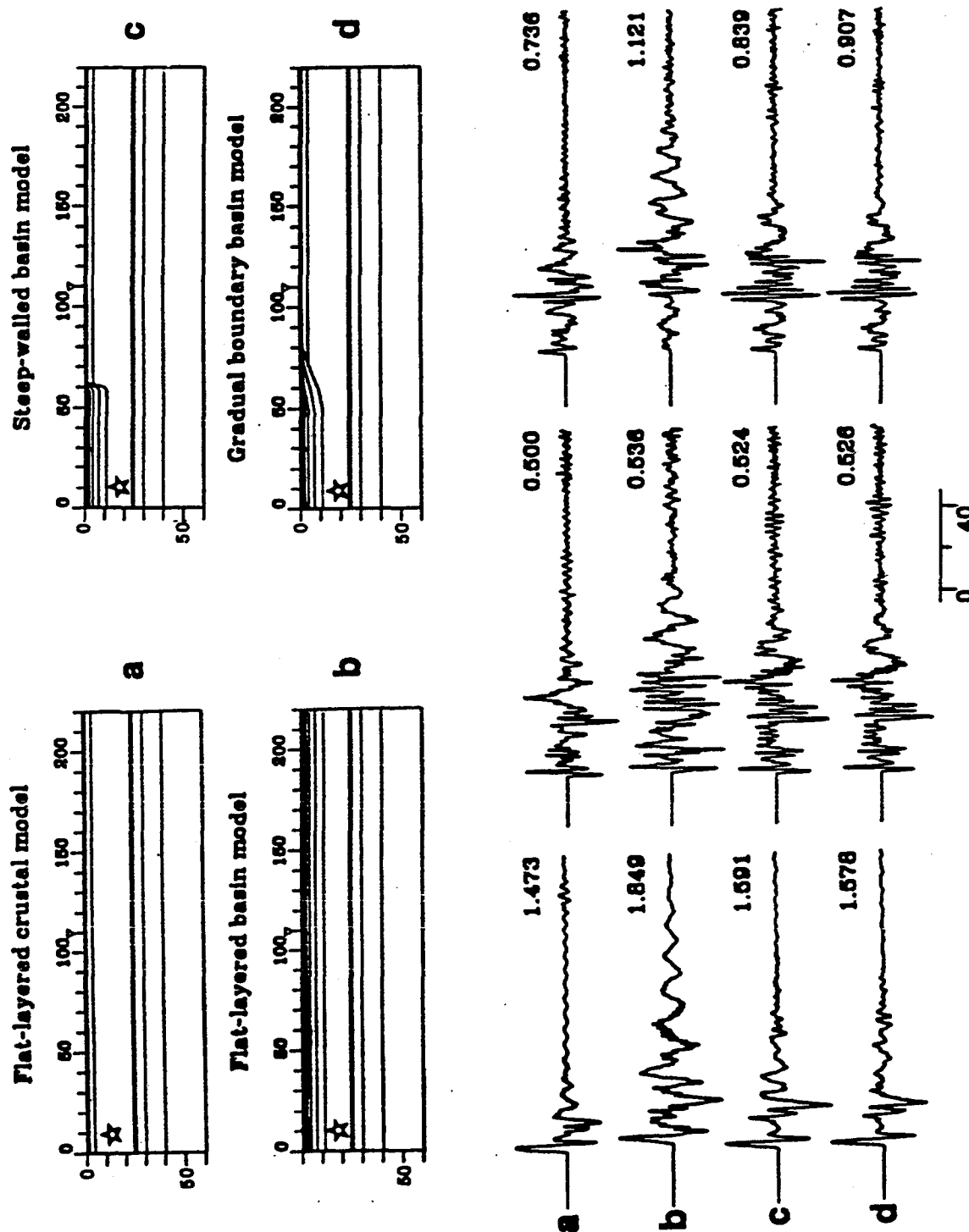
Figure 4. Four crustal models (upper panel) and corresponding three-component seismograms (lower panel) computed with finite difference method, assuming a strike-slip source. The source location is indicated by a star and the receiver is indicated by a triangle $\Delta = 100$ km, after Song et al., (1995).
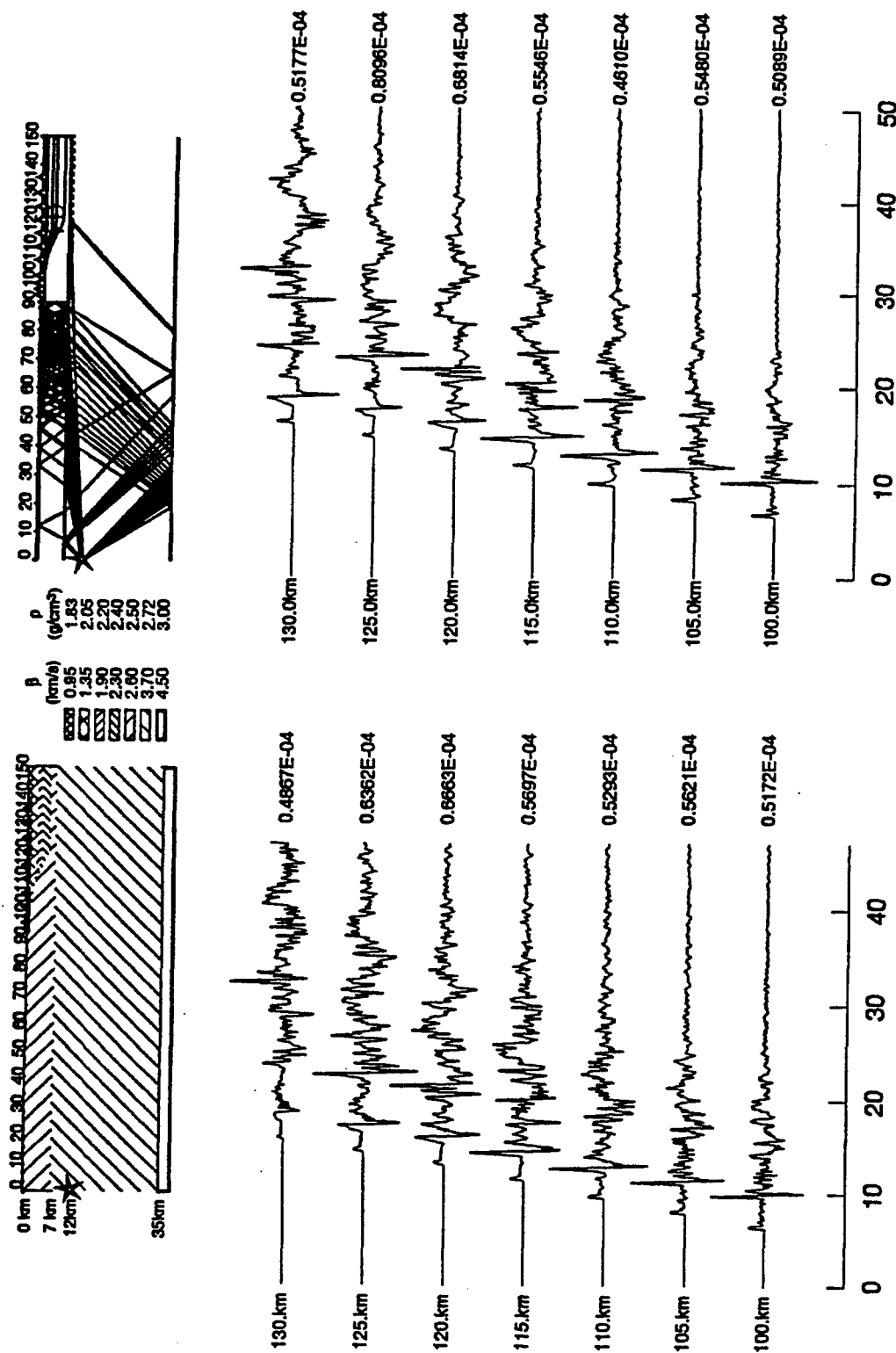
Figure 5. Comparison of synthetics generated by two finite-difference codes for a set of stations crossing the edge of a basin (actually Los Angeles basin, Scrivner & Helmberger, 1994). Those on the left generated the entire distance by FD (Vidale & Helmberger) while the profile on the right contains the results of interfacing the analytical solution with FD at the box boundary (Wen & Helmberger, 1995).